DOI: 10.1148/rg.266065025

RadioGraphics 2006;26:1719-1734

EDUCATION EXHIBIT

Patterns of Enhancement on Breast MR Images: Interpretation and Imaging Pitfalls[1]

Katarzyna J. Macura, MD, PhD, Ronald Ouwerkerk, PhD, Michael A. Jacobs, PhD and David A. Bluemke, MD, PhD

[1] From the Russell H. Morgan Department of Radiology and Radiological Sciences (K.J.M., R.O., M. A.J., D.A.B.) and Sidney Kimmel Cancer Center, Department of Oncology (M.A.J.), Johns Hopkins Medical Institutions, 600 N Wolfe St, BLA-B 179 RAD, Baltimore, MD 21287. Presented as an education exhibit at the 2005 RSNA Annual Meeting. Received March 15, 2006; revision requested April 12 and received May 23; accepted May 31. M.A.J. supported by grants NIH 1R01CA100184 and P50 CA103175. R.O. supported by grant 5R21CA095907. All authors have no financial relationships to disclose. **Address correspondence to** K.J.M. (e-mail: kmacura@jhmi.edu).

Abstract

The role of dynamic contrast material–enhanced magnetic resonance (MR) imaging of the breast as an adjunct to the conventional techniques of mammography and ultrasonography has been established in numerous research studies. MR imaging improves the detection and characterization of primary and recurrent breast cancers and allows evaluation of the response to therapy. The breast imaging lexicon published by the American College of Radiology allows a standardized and consistent description of the morphologic and kinetic characteristics of breast lesions; however, there are many challenges in the interpretation of breast enhancement patterns and kinetics, and many imaging and interpretation pitfalls must be considered. New breast MR imaging techniques that are based on the use of molecular markers of malignancy may help improve lesion characterization. The margin characteristics of a lesion and the intensity of its enhancement at MR imaging 2 minutes or less after contrast material injection are currently considered the most important features for breast lesion diagnosis.

LEARNING OBJECTIVES

After reading this article and taking the test, the reader will be able to:

- Describe the different enhancement patterns in lesions on breast MR images and the predictive value of each pattern for cancer detection.
- Recognize the enhancement kinetics that help determine whether a breast lesion is benign or malignant.
- Discuss diagnostic and technical pitfalls of breast MR imaging.

Introduction

Dynamic contrast material–enhanced magnetic resonance (MR) imaging of the breast is increasingly used as an adjunct to mammography and ultrasonography (US) to improve the detection and characterization of primary and recurrent breast cancers and for evaluation of the response to therapy. MR imaging is useful for detecting multifocality and multicentricity of breast cancer; differentiating between scar tissue and recurrent cancer after breast-conserving therapy (1); screening patients in high-risk groups (eg, those with the *BRCA1* gene) (2); examining breasts that contain implants; examining the breasts of patients with histologically proved metastatic breast cancer with unknown primary origin (3); and, in patients with a finding of cancer in one breast, screening the contralateral breast for occult cancer (4). The sensitivity of MR imaging for the detection of breast cancer is very high, with 90% being the value reported in most studies (5,6). However, with regard to the detection of ductal carcinoma in situ (DCIS), the sensitivity of MR imaging varies between 40% and 100% (7). The result may be false-negative in the presence of DCIS or an invasive ductal or lobular malignancy. Specificity of 37%–100% has been reported for breast MR imaging; in most studies, it has varied from 50% to 70% (5). The relatively low specificity of breast MR imaging is a disadvantage, and rigorous criteria have been proposed for the interpretation of breast MR images (8). In addition, new imaging techniques based on molecular and cellular properties of tissues have been investigated (9,10). The use of computer-assisted methods such as neural network clustering has been proposed to aid in the assessment of contrast enhancement on breast MR images (11).

The American College of Radiology breast MR imaging lexicon provides a specific standardized vocabulary for describing the morphologic and kinetic characteristics of breast lesions (8). All suspicious areas are defined as a focus or foci (with a diameter of less than 5 mm), mass (a three-dimensional space-occupying lesion with a convex margin), or nonmass. The description of a mass should include a characterization of its shape (round, oval, lobular, irregular), margin (smooth, irregular, spiculated), and internal enhancement pattern (homogeneous, heterogeneous, rimlike, central, septal). The description of a nonmass lesion should include a characterization of its distribution (focal or multifocal, linear, ductal, segmental, regional, multiregional, diffuse), internal enhancement (homogeneous, heterogeneous, stippled, clumped, reticular), and symmetry. Associated findings such as edema, adenopathy, cysts, and skin and chest wall involvement are reported as well. The kinetic curve assessment involves a description of both the initial peak (slow, medium, rapid) and the delayed phase (persistent, plateau, or washout) of contrast enhancement.

In this article, we discuss the different patterns of enhancement, each of which has a specific meaning with regard to the diagnosis of breast abnormalities. The discussion is based on the results of several research studies in which the predictive value of particular imaging features was investigated during the interpretation of contrast-enhanced breast MR images. We also focus on potential diagnostic and technical pitfalls of breast MR imaging and discuss emerging techniques that are aimed at improving lesion characterization with the use of molecular markers of malignancy.

Enhancement Patterns

Lack of Enhancement

Teaching Point The absence of a visible lesion on contrast-enhanced MR images that corresponds to a palpable or mammographically visible abnormality is highly predictive of a benign finding. However, the absence of observed enhancement at breast MR imaging does not exclude in situ or invasive cancer. Many invasive cancers that show no enhancement are small or have a small invasive component (12). Lack of enhancement has a high negative predictive value (NPV) for malignancy (88%–96%) (12,13). Among nonenhancing tumors, about 48% are DCIS (7,12), and 52% are invasive carcinomas (12,13).

Morphologic Criteria for Benignity

Many benign breast lesions may appear enhanced, including nonproliferative lesions (mild hyperplasia, fibroadenomas), proliferative lesions without atypia (sclerosing adenosis, radial and complexing sclerosing lesions, moderate hyperplasia, intraductal papillomas), and atypical lobular and ductal hyperplasia. The normal breast parenchyma, especially in premenopausal women, also may appear focally enhanced, and this appearance may lead to a false-positive finding (14).

A typical benign feature for masses is a smooth margin (NPV, 95%). Low-signal-intensity internal septa were demonstrated to be predictive of benignity (NPV, 98%) (13) (Fig 1). However, recent results of a study by Schnall et al revealed that 47% of malignant lesions were shown to have nonenhancing internal septa (12). If a mass is lobulated and shows no enhancement or only minimal enhancement, it is likely benign (NPV, 100%) (13). If a mass is lobulated and shows moderate to marked enhancement (NPV, 67%), further evaluation may be warranted (13). Correlation between the enhancing portion of the lesion and its T2-weighted signal intensity is helpful (15). T2-weighted signal hyperintensity in the same portion of the lesion that appears enhanced on T1-weighted images is highly suggestive of benignity, although not all masses with high signal intensity on T2-weighted images are benign. A finding of mild regional nonmass enhancement also is suggestive of a benign abnormality (NPV, 92%).

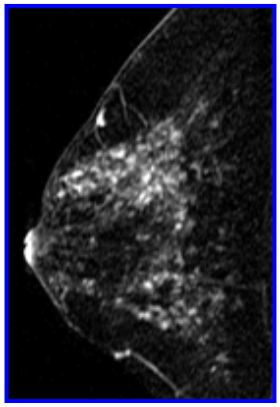

View larger version (98K):
[in this window]
[in a new window]
[Download PPT slide]

Figure 1a. Benign features. **(a, b)** Contrast-enhanced T1-weighted fat-saturated gradient-echo (GRE) (repetition time msec/echo time msec, 20/4.5; flip angle, 30°) images from a 51-year-old woman show regional micronodular (<5 mm stippled or punctate) enhancement in fibrocystic breast tissue **(a)** and rimlike enhancement around a cyst (arrow in **b**) within a region of fibrocystic breast tissue. **(c)** T2-weighted (4000/90) fat-saturated image (same patient as in **a** and **b**) shows the cyst (arrow). Comparison of the contrast-enhanced images with the T2-weighted image is important to recognize the benign nature of these findings. **(d)** Contrast-enhanced T1-weighted GRE (20/4.5; flip angle, 30°) subtraction image from a 44-year-old woman shows an oval mass with smooth and lobular margins and enhancement with dark internal septa, typical of a fibroadenoma (arrow). **(e)** T2-weighted (4000/90) fat-saturated image (same patient as in **d**) shows increased signal intensity in the lesion (arrow) in comparison with that seen in **d**. Increased T2-weighted signal intensity is typical of a myxoid fibroadenoma in a woman of this age. In women older than 50 years, age-related sclerotic changes in fibroadenomas result in a greater prevalence of lesions with fibrotic low signal intensity, which reduces the diagnostic usefulness of the T2-weighted imaging characteristic.

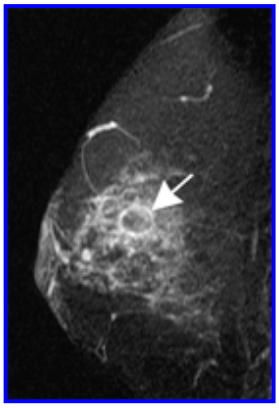

View larger version (116K):
[in this window]
[in a new window]
[Download PPT slide]

Figure 1b. Benign features. **(a, b)** Contrast-enhanced T1-weighted fat-saturated gradient-echo (GRE) (repetition time msec/echo time msec, 20/4.5; flip angle, 30°) images from a 51-year-old woman show regional micronodular (<5 mm stippled or punctate) enhancement in fibrocystic breast tissue **(a)** and rimlike enhancement around a cyst (arrow in **b**) within a region of fibrocystic breast tissue. **(c)** T2-weighted (4000/90) fat-saturated image (same patient as in **a** and **b**) shows the cyst (arrow). Comparison of the contrast-enhanced images with the T2-weighted image is important to recognize the benign nature of these findings. **(d)** Contrast-enhanced T1-weighted GRE (20/4.5; flip angle, 30°) subtraction image from a 44-year-old woman shows an oval mass with smooth and lobular margins and enhancement with dark internal septa, typical of a fibroadenoma (arrow). **(e)** T2-weighted (4000/90) fat-saturated image (same patient as in **d**) shows increased signal intensity in the lesion (arrow) in comparison with that seen in **d**. Increased T2-weighted signal intensity is typical of a myxoid fibroadenoma in a woman of this age. In women older than 50 years, age-related sclerotic changes in fibroadenomas result in a greater prevalence of lesions with fibrotic low signal intensity, which reduces the diagnostic usefulness of the T2-weighted imaging characteristic.

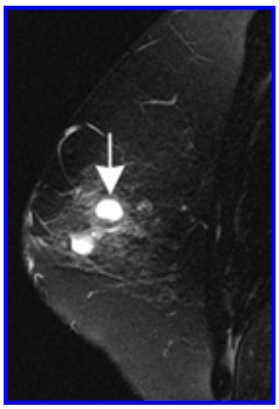

View larger version (101K):
[in this window]
[in a new window]
[Download PPT slide]

Figure 1c. Benign features. **(a, b)** Contrast-enhanced T1-weighted fat-saturated gradient-echo (GRE) (repetition time msec/echo time msec, 20/4.5; flip angle, 30°) images from a 51-year-old woman show regional micronodular (<5 mm stippled or punctate) enhancement in fibrocystic breast tissue **(a)** and rimlike enhancement around a cyst (arrow in **b**) within a region of fibrocystic breast tissue. **(c)** T2-weighted (4000/90) fat-saturated image (same patient as in **a** and **b**) shows the cyst (arrow). Comparison of the contrast-enhanced images with the T2-weighted image is important to recognize the benign nature of these findings. **(d)** Contrast-enhanced T1-weighted GRE (20/4.5; flip angle, 30°) subtraction image from a 44-year-old woman shows an oval mass with smooth and lobular margins and enhancement with dark internal septa, typical of a fibroadenoma (arrow). **(e)** T2-weighted (4000/90) fat-saturated image (same patient as in **d**) shows increased signal intensity in the lesion (arrow) in comparison with that seen in **d**. Increased T2-weighted signal intensity is typical of a myxoid fibroadenoma in a woman of this age. In women older than 50 years, age-related sclerotic changes in fibroadenomas result in a greater prevalence of lesions with fibrotic low signal intensity, which reduces the diagnostic usefulness of the T2-weighted imaging characteristic.

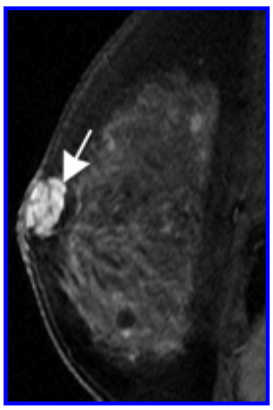

View larger version (100K):
[in this window]
[in a new window]
[Download PPT slide]

Figure 1d. Benign features. **(a, b)** Contrast-enhanced T1-weighted fat-saturated gradient-echo (GRE) (repetition time msec/echo time msec, 20/4.5; flip angle, 30°) images from a 51-year-old woman show regional micronodular (<5 mm stippled or punctate) enhancement in fibrocystic breast tissue **(a)** and rimlike enhancement around a cyst (arrow in **b**) within a region of fibrocystic breast tissue. **(c)** T2-weighted (4000/90) fat-saturated image (same patient as in **a** and **b**) shows the cyst (arrow). Comparison of the contrast-enhanced images with the T2-weighted image is important to recognize the benign nature of these findings. **(d)** Contrast-enhanced T1-weighted GRE (20/4.5; flip angle, 30°) subtraction image from a 44-year-old woman shows an oval mass with smooth and lobular margins and enhancement with dark internal septa, typical of a fibroadenoma (arrow). **(e)** T2-weighted (4000/90) fat-saturated image (same patient as in **d**) shows increased signal intensity in the lesion (arrow) in comparison with that seen in **d**. Increased T2-weighted signal intensity is typical of a myxoid fibroadenoma in a woman of this age. In women older than 50 years, age-related sclerotic changes in fibroadenomas result in a greater prevalence of lesions with fibrotic low signal intensity, which reduces the diagnostic usefulness of the T2-weighted imaging characteristic.

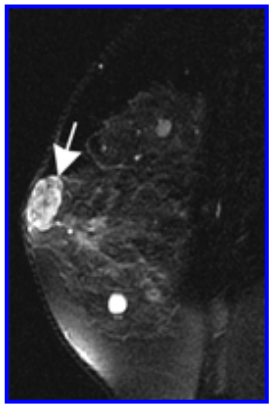

View larger version (98K):
[in this window]
[in a new window]
[Download PPT slide]

Figure 1e. Benign features. **(a, b)** Contrast-enhanced T1-weighted fat-saturated gradient-echo (GRE) (repetition time msec/echo time msec, 20/4.5; flip angle, 30°) images from a 51-year-old woman show regional micronodular (<5 mm stippled or punctate) enhancement in fibrocystic breast tissue **(a)** and rimlike enhancement around a cyst (arrow in **b**) within a region of fibrocystic breast tissue. **(c)** T2-weighted (4000/90) fat-saturated image (same patient as in **a** and **b**) shows the cyst (arrow). Comparison of the contrast-enhanced images with the T2-weighted image is important to recognize the benign nature of these findings. **(d)** Contrast-enhanced T1-weighted GRE (20/4.5; flip angle, 30°) subtraction image from a 44-year-old woman shows an oval mass with smooth and lobular margins and enhancement with dark internal septa, typical of a fibroadenoma (arrow). **(e)** T2-weighted (4000/90) fat-saturated image (same patient as in **d**) shows increased signal intensity in the lesion (arrow) in comparison with that seen in **d**. Increased T2-weighted signal intensity is typical of a myxoid fibroadenoma in a woman of this age. In women older than 50 years, age-related sclerotic changes in fibroadenomas result in a greater prevalence of lesions with fibrotic low signal intensity, which reduces the diagnostic usefulness of the T2-weighted imaging characteristic.

Morphologic Criteria for Malignancy

Teaching Point The description of the margin of a focal mass is the most predictive feature of the breast MR image interpretation. Irregular or spiculated margins have a positive predictive value (PPV) of 84%–91% (13) (Fig 2). Rimlike enhancement highly correlates with a cancer diagnosis (PPV, 84%) (12); however, this feature is uncommon, with a prevalence of 16%. Other features associated with malignancy include heterogeneous internal enhancement and enhancing internal septa.

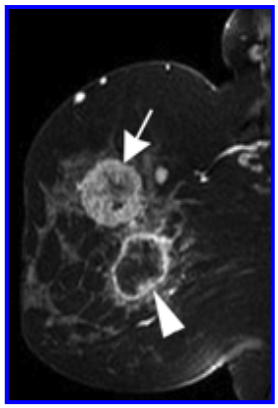

View larger version (87K):
[in this window]
[in a new window]
[Download PPT slide]

Figure 2a. Malignant features. **(a)** Contrast-enhanced T1-weighted fat-saturated GRE (20/4.5; flip angle, 30°) image shows two masses in the left breast of a 44-year-old woman, one with thin rimlike enhancement at the 4-o'clock position (arrowhead) and the other with heterogeneous enhancement and enhanced internal septa at the 2-o'clock position (arrow). **(b)** T2-weighted (4000/90) fat-saturated image (same patient as in **a)** shows low signal intensity in the portions of the masses that appeared enhanced in **a**. A central region of necrosis in the mass at the 4-o'clock position shows increased internal T2-weighted signal intensity. The masses proved to be poorly differentiated ductal carcinoma with necrosis and signet ring cell features. **(c)** Contrast-enhanced T1-weighted GRE (20/4.5; flip angle, 30°) subtraction image from a 42-year-old woman shows a spiculated margin in an infiltrating carcinoma with ductal and lobular features. **(d)** Contrast-enhanced T1-weighted fat-saturated GRE (20/4.5; flip angle, 30°) image from a 52-year-old woman shows a retroareolar mass (arrow) with an irregular margin and heterogeneous enhancement. The results of histologic analysis indicated infiltrating ductal carcinoma. **(e)** T2-weighted (4000/90) fat-saturated image (same patient as in **d**) shows the mass (arrow) with low signal intensity. Note the focal skin thickening and nipple retraction.

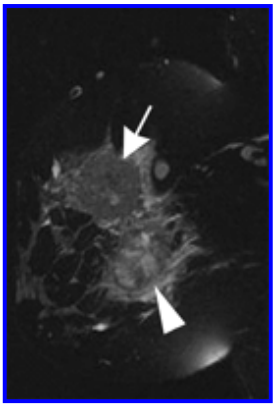

View larger version (80K):
[in this window]
[in a new window]
[Download PPT slide]

Figure 2b. Malignant features. **(a)** Contrast-enhanced T1-weighted fat-saturated GRE (20/4.5; flip angle, 30°) image shows two masses in the left breast of a 44-year-old woman, one with thin rimlike enhancement at the 4-o'clock position (arrowhead) and the other with heterogeneous enhancement and enhanced internal septa at the 2-o'clock position (arrow). **(b)** T2-weighted (4000/90) fat-saturated image (same patient as in **a)** shows low signal intensity in the portions of the masses that appeared enhanced in **a**. A central region of necrosis in the mass at the 4-o'clock position shows increased internal T2-weighted signal intensity. The masses proved to be poorly differentiated ductal carcinoma with necrosis and signet ring cell features. **(c)** Contrast-enhanced T1-weighted GRE (20/4.5; flip angle, 30°) subtraction image from a 42-year-old woman shows a spiculated margin in an infiltrating carcinoma with ductal and lobular features. **(d)** Contrast-enhanced T1-weighted fat-saturated GRE (20/4.5; flip angle, 30°) image from a 52-year-old woman shows a retroareolar mass (arrow) with an irregular margin and heterogeneous enhancement. The results of histologic analysis indicated infiltrating ductal carcinoma. **(e)** T2-weighted (4000/90) fat-saturated image (same patient as in **d**) shows the mass (arrow) with low signal intensity. Note the focal skin thickening and nipple retraction.

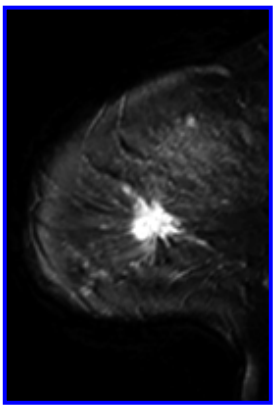

View larger version (64K):
[in this window]
[in a new window]
[Download PPT slide]

Figure 2c. Malignant features. **(a)** Contrast-enhanced T1-weighted fat-saturated GRE (20/4.5; flip angle, 30°) image shows two masses in the left breast of a 44-year-old woman, one with thin rimlike enhancement at the 4-o'clock position (arrowhead) and the other with heterogeneous enhancement and enhanced internal septa at the 2-o'clock position (arrow). **(b)** T2-weighted (4000/90) fat-saturated image (same patient as in **a)** shows low signal intensity in the portions of the masses that appeared enhanced in **a**. A central region of necrosis in the mass at the 4-o'clock position shows increased internal T2-weighted signal intensity. The masses proved to be poorly differentiated ductal carcinoma with necrosis and signet ring cell features. **(c)** Contrast-enhanced T1-weighted GRE (20/4.5; flip angle, 30°) subtraction image from a 42-year-old woman shows a spiculated margin in an infiltrating carcinoma with ductal and lobular features. **(d)** Contrast-enhanced T1-weighted fat-saturated GRE (20/4.5; flip angle, 30°) image from a 52-year-old woman shows a retroareolar mass (arrow) with an irregular margin and heterogeneous enhancement. The results of histologic analysis indicated infiltrating ductal carcinoma. **(e)** T2-weighted (4000/90) fat-saturated image (same patient as in **d**) shows the mass (arrow) with low signal intensity. Note the focal skin thickening and nipple retraction.

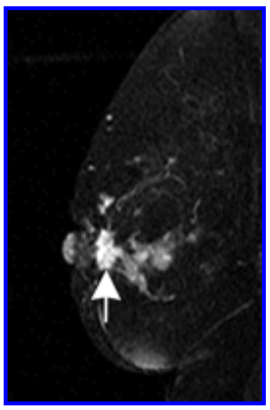

View larger version (72K):
[in this window]
[in a new window]
[Download PPT slide]

Figure 2d. Malignant features. **(a)** Contrast-enhanced T1-weighted fat-saturated GRE (20/4.5; flip angle, 30°) image shows two masses in the left breast of a 44-year-old woman, one with thin rimlike enhancement at the 4-o'clock position (arrowhead) and the other with heterogeneous enhancement and enhanced internal septa at the 2-o'clock position (arrow). **(b)** T2-weighted (4000/90) fat-saturated image (same patient as in **a)** shows low signal intensity in the portions of the masses that appeared enhanced in **a**. A central region of necrosis in the mass at the 4-o'clock position shows increased internal T2-weighted signal intensity. The masses proved to be poorly differentiated ductal carcinoma with necrosis and signet ring cell features. **(c)** Contrast-enhanced T1-weighted GRE (20/4.5; flip angle, 30°) subtraction image from a 42-year-old woman shows a spiculated margin in an infiltrating carcinoma with ductal and lobular features. **(d)** Contrast-enhanced T1-weighted fat-saturated GRE (20/4.5; flip angle, 30°) image from a 52-year-old woman shows a retroareolar mass (arrow) with an irregular margin and heterogeneous enhancement. The results of histologic analysis indicated infiltrating ductal carcinoma. **(e)** T2-weighted (4000/90) fat-saturated image (same patient as in **d**) shows the mass (arrow) with low signal intensity. Note the focal skin thickening and nipple retraction.

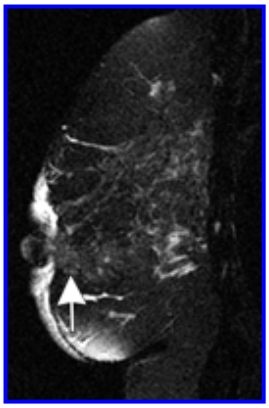

View larger version (107K):
[in this window]
[in a new window]
[Download PPT slide]

Figure 2e. Malignant features. **(a)** Contrast-enhanced T1-weighted fat-saturated GRE (20/4.5; flip angle, 30°) image shows two masses in the left breast of a 44-year-old woman, one with thin rimlike enhancement at the 4-o'clock position (arrowhead) and the other with heterogeneous enhancement and enhanced internal septa at the 2-o'clock position (arrow). **(b)** T2-weighted (4000/90) fat-saturated image (same patient as in **a)** shows low signal intensity in the portions of the masses that appeared enhanced in **a**. A central region of necrosis in the mass at the 4-o'clock position shows increased internal T2-weighted signal intensity. The masses proved to be poorly differentiated ductal carcinoma with necrosis and signet ring cell features. **(c)** Contrast-enhanced T1-weighted GRE (20/4.5; flip angle, 30°) subtraction image from a 42-year-old woman shows a spiculated margin in an infiltrating carcinoma with ductal and lobular features. **(d)** Contrast-enhanced T1-weighted fat-saturated GRE (20/4.5; flip angle, 30°) image from a 52-year-old woman shows a retroareolar mass (arrow) with an irregular margin and heterogeneous enhancement. The results of histologic analysis indicated infiltrating ductal carcinoma. **(e)** T2-weighted (4000/90) fat-saturated image (same patient as in **d**) shows the mass (arrow) with low signal intensity. Note the focal skin thickening and nipple retraction.

A linear or branching ductal distribution of enhancement is difficult to assess and interobserver agreement is poor, according to a report by the MR imaging lexicon committee (16), and the reported PPV for this feature has varied from 24% to 85% (5).

A moderate to marked degree of nonmass regional enhancement has a PPV of 59% (13). Regional enhancement with a micronodular (stippled) pattern was found in both benign (eg, fibrocystic disease) and malignant (eg, DCIS) abnormalities (13). Stippled enhancement is associated with a low incidence of malignancy (25%), while clumped, heterogeneous, and homogeneous enhancement are associated with a 60%, 53%, and 67% likelihood of cancer, respectively (12). Regional enhancement associated with a focal lesion was shown to have a PPV of 81%; however, this finding has a low prevalence and is seen in only 14% of patients with a focal malignancy. A segmental distribution of enhancement was associated with a 78% likelihood of cancer, while a regional distribution was associated with a 21% likelihood of cancer. Therefore, mild stippled enhancement with a regional distribution is indicative of benignity, whereas segmental or clumped enhancement is more likely to indicate malignancy (12).

Other Features

T2-weighted Signal Characteristics

Teaching Point T2-weighted signal hyperintensity within the viable (enhancing) portion of the lesion is highly suggestive of benign histology (15). However, T2-weighted signal intensity is not a reliable predictor of benignity in irregular or spiculated masses. Colloid (mucinous) carcinoma may be manifested as a hyperintense and minimally enhancing mass on T2-weighted images (13,17). On T2-weighted images, breast cancers are more likely (87%) to have iso- or hypointense signal, compared to the signal intensity of the normal breast parenchyma (Fig 2) (18). Hypointense internal septa on T2-weighted images are typical of benign fibroadenomas (Fig 1). Rarely, adenoid cystic carcinoma may contain low-signal-intensity septa that are nonenhanced (13).

The assessment of lesions on T2-weighted images is most helpful in younger patients. Myxoid fibroadenomas in young women typically demonstrate increased T2-weighted signal intensity. However, there are age-related sclerotic changes in fibroadenomas in older women, and the greater prevalence of fibrotic low-signal-intensity fibroadenomas in women older than 50 years reduces the diagnostic value of the T2-weighted signal intensity criterion (18). Sclerotic fibroadenomas may have the same hypointense appearance as well-circumscribed breast cancers. However, with the progression of fibrosis, the enhancement rate of fibroadenomas decreases. Thus, the primary diagnostic criterion of enhancement may be used to avoid unnecessary referral for biopsy. Medullary cancers tend to occur in younger women and may have a circumscribed appearance. The signal intensity of the lesion on T2-weighted

images may not aid in the differential diagnosis of myxoid fibroadenoma and medullary cancer. For these reasons, the T2-weighted signal intensity of a breast lesion is used as a secondary criterion, to confirm a diagnosis of benignity established on the basis of morphologic features (the primary criterion), and not to rule out breast cancer.

Focal Perilesional Edema

A focal area of hyperintense T2-weighted signal near a lesion is highly suggestive of malignancy. The signal intensity increase is thought to be related to increased capillary permeability in the presence of tumor-related angiogenesis (15).

Architectural Distortion

An architectural distortion that is nonenhanced may represent a radial scar; if enhanced, it is highly suggestive of invasive cancer. Desmoplastic tethering (the hook sign) has been described as highly indicative of a malignancy in an untreated breast (15). This feature, which is thought to represent invasion of the Cooper ligaments in the direction of the pectoral muscle, is best evaluated on T2-weighted images. The hook sign is not observed in the presence of noninvasive cancers.

Skin Thickening and Edema

Skin thickening and edema in an untreated breast on MR images, as on mammograms, may be signs of malignancy, especially of inflammatory carcinoma. In a treated breast, these features are frequently observed after radiation therapy.

Lymph Nodes

The lack of visibility or the subtle visibility of axillary lymph nodes is almost as commonly associated with benign lesions as with malignant ones. Therefore, the absence of adenopathy does not help differentiate benignity from malignancy. In contrast, nodes with a diameter of more than 1 cm are more common in malignant cases (15). In addition, a loss of the fatty hilum of the lymph node is suggestive of malignant involvement.

Enhancement Kinetics

Breast lesion enhancement can be characterized qualitatively by assessing the enhancement kinetics curve obtained by plotting the signal intensity values in breast tissue intensity over time after contrast material injection. These curves show both the initial slope of increasing enhancement, from the baseline value to the peak, and the subsequent trend. Three enhancement patterns can be identified on the basis of the signal intensity–time curve.

Type I is a pattern of progressive enhancement, with a continuous increase in signal intensity on each successive contrast-enhanced image (Fig 3). This enhancement pattern is usually associated with a benign finding (83% benign, 9% malignant) (19). Its sensitivity and specificity for indication of a benign lesion are 52.2% and 71%, respectively (6). However, Schnall et al reported that readers in a multiinstitutional trial described the enhancement kinetics as persistent in 45% of lesions that proved to be cancers (12).

Figure 3a. Type I enhancement curve in a lesion stable over 2 years. The patient, a 28-year-old woman, had contralateral breast cancer (Fig 6). **(a)** Contrast-enhanced T1-weighted GRE (20/4.5; flip angle, 30°) subtraction image shows an 8-mm-diameter mass (arrow) with minimal lobulation and enhancement. **(b)** T2-weighted (4000/90) fat-saturated image shows an area of high signal intensity (arrow) within the lesion. **(c)** Curve indicates progressive enhancement in the lesion. The vertical axis indicates the percentage of enhancement, and the horizontal axis indicates the time in seconds.

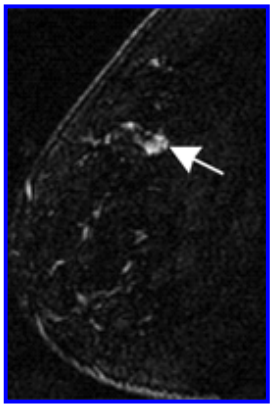

View larger version (93K):
[in this window]
[in a new window]
[Download PPT slide]

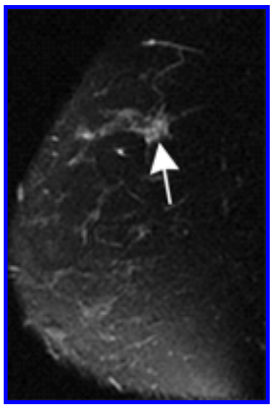

View larger version (92K):
[in this window]
[in a new window]
[Download PPT slide]

Figure 3b. Type I enhancement curve in a lesion stable over 2 years. The patient, a 28-year-old woman, had contralateral breast cancer (Fig 6). **(a)** Contrast-enhanced T1-weighted GRE (20/4.5; flip angle, 30°) subtraction image shows an 8-mm-diameter mass (arrow) with minimal lobulation and enhancement. **(b)** T2-weighted (4000/90) fat-saturated image shows an area of high signal intensity (arrow) within the lesion. **(c)** Curve indicates progressive enhancement in the lesion. The vertical axis indicates the percentage of enhancement, and the horizontal axis indicates the time in seconds.

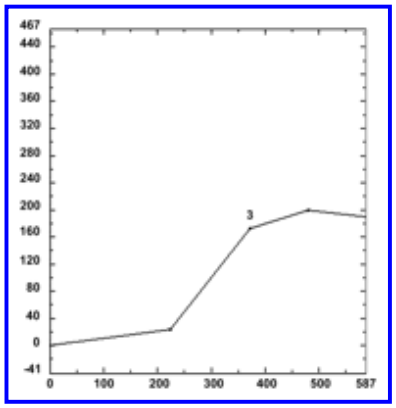

View larger version (12K):
[in this window]
[in a new window]
[Download PPT slide]

Figure 3c. Type I enhancement curve in a lesion stable over 2 years. The patient, a 28-year-old woman, had contralateral breast cancer (Fig 6). **(a)** Contrast-enhanced T1-weighted GRE (20/4.5; flip angle, 30°) subtraction image shows an 8-mm-diameter mass (arrow) with minimal lobulation and enhancement. **(b)** T2-weighted (4000/90) fat-saturated image shows an area of high signal intensity (arrow) within the lesion. **(c)** Curve indicates progressive enhancement in the lesion. The vertical axis indicates the percentage of enhancement, and the horizontal axis indicates the time in seconds.

Type II is a plateau pattern, in which an initial increase in signal intensity is followed by a flattening of the enhancement curve (Fig 4). This pattern has a sensitivity of 42.6% and specificity of 75% for the detection of malignancy (6).

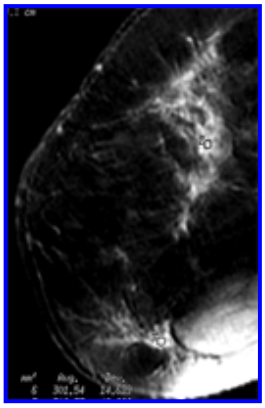

View larger version (82K):
[in this window]
[in a new window]
[Download PPT slide]

Figure 4a. Type II curve in a multifocal and bilateral invasive lobular carcinoma in a 39-year-old woman. **(a)** Contrast-enhanced T1-weighted fat-saturated GRE (20/4.5; flip angle, 30°) image shows regional nonmass enhancement. **(b)** Color-coded map shows foci with the maximum slope of enhancement increase (red) after contrast material injection. Two foci were selected as regions of interest (ROIs). **(c)** Curves indicate plateau enhancement. The vertical axis indicates the percentage of enhancement, and the horizontal axis indicates the time in minutes.

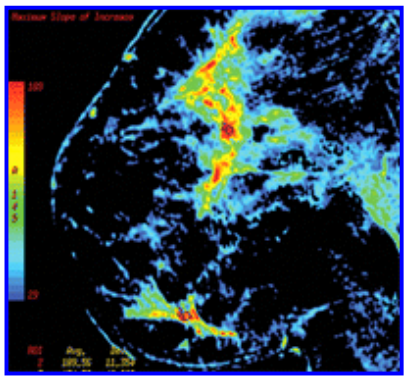

View larger version (86K):
[in this window]
[in a new window]
[Download PPT slide]

Figure 4b. Type II curve in a multifocal and bilateral invasive lobular carcinoma in a 39-year-old woman. **(a)** Contrast-enhanced T1-weighted fat-saturated GRE (20/4.5; flip angle, 30°) image shows regional nonmass enhancement. **(b)** Color-coded map shows foci with the maximum slope of enhancement increase (red) after contrast material injection. Two foci were selected as regions of interest (ROIs). **(c)** Curves indicate plateau enhancement. The vertical axis indicates the percentage of enhancement, and the horizontal axis indicates the time in minutes.

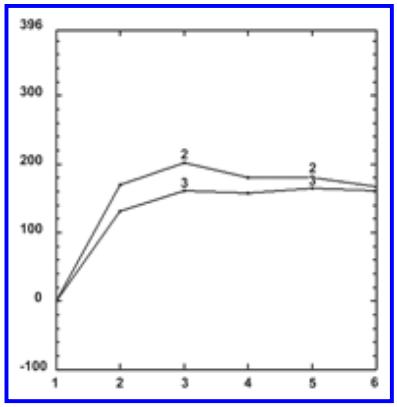

Figure 4c. Type II curve in a multifocal and bilateral invasive lobular carcinoma in a 39-year-old woman. **(a)** Contrast-enhanced T1-weighted fat-saturated GRE (20/4.5; flip angle, 30°) image shows regional nonmass enhancement. **(b)** Color-coded map shows foci with the maximum slope of enhancement increase (red) after contrast material injection. Two foci were selected as regions of interest (ROIs). **(c)** Curves indicate plateau enhancement. The vertical axis indicates the percentage of enhancement, and the horizontal axis indicates the time in minutes.

View larger version (12K):
[in this window]
[in a new window]
[Download PPT slide]

Type III, a washout enhancement pattern, involves an initial increase and subsequent decrease in signal intensity (Figs 5, 6). This pattern is not usually seen in patients with benign lesions (specificity, 90.4%), but it has a sensitivity of only 20.5% (6). Schnall et al reported that 76% of curves that showed a washout pattern were associated with cancer. Both type II and type III curves should be considered suggestive of malignancy.

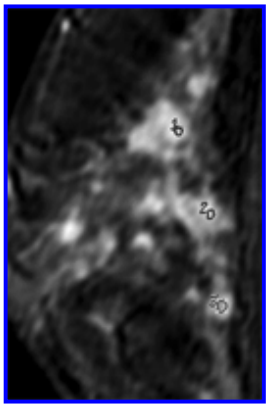

View larger version (99K):
[in this window]
[in a new window]
[Download PPT slide]

Figure 5a. Type III curve from multifocal infiltrating lobular carcinoma in a 40-year-old woman. **(a)** Contrast-enhanced T1-weighted fat-saturated GRE (20/4.5; flip angle, 30°) image shows regions of clumped nonmasslike enhancement in all four quadrants. **(b)** Color-coded map of the maximum slope of enhancement shows three ROIs selected in areas of rapid peak enhancement (red). **(c)** Enhancement curves indicate early washout. The vertical axis indicates the percentage of enhancement, and the horizontal axis indicates the time in minutes.

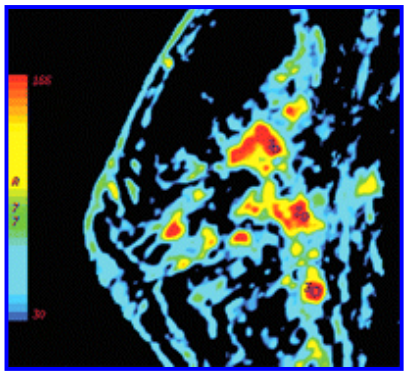

View larger version (95K):
[in this window]
[in a new window]
[Download PPT slide]

Figure 5b. Type III curve from multifocal infiltrating lobular carcinoma in a 40-year-old woman. **(a)** Contrast-enhanced T1-weighted fat-saturated GRE (20/4.5; flip angle, 30°) image shows regions of clumped nonmasslike enhancement in all four quadrants. **(b)** Color-coded map of the maximum slope of enhancement shows three ROIs selected in areas of rapid peak enhancement (red). **(c)** Enhancement curves indicate early washout. The vertical axis indicates the percentage of enhancement, and the horizontal axis indicates the time in minutes.

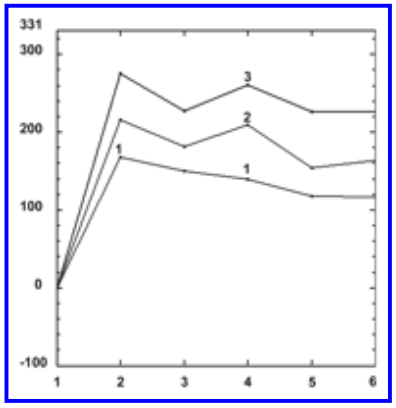

View larger version (16K):
[in this window]
[in a new window]
[Download PPT slide]

Figure 5c. Type III curve from multifocal infiltrating lobular carcinoma in a 40-year-old woman. **(a)** Contrast-enhanced T1-weighted fat-saturated GRE (20/4.5; flip angle, 30°) image shows regions of clumped nonmasslike enhancement in all four quadrants. **(b)** Color-coded map of the maximum slope of enhancement shows three ROIs selected in areas of rapid peak enhancement (red). **(c)** Enhancement curves indicate early washout. The vertical axis indicates the percentage of enhancement, and the horizontal axis indicates the time in minutes.

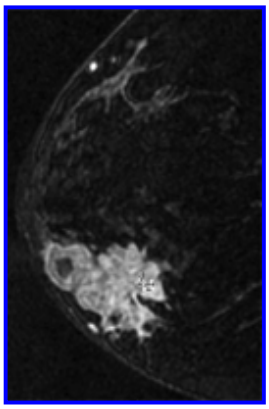

View larger version (88K):
[in this window]
[in a new window]
[Download PPT slide]

Figure 6a. Moderately to poorly differentiated palpable mass (infiltrating ductal carcinoma) in a 28-year-old woman, 3 months postpartum. **(a)** Contrast-enhanced T1-weighted fat-saturated GRE (20/4.5; flip angle, 30°) image shows an irregular mass with an irregular and spiculated margin, features typical of invasive carcinoma. **(b)** T2-weighted (4000/90) fat-saturated image shows a region of low signal intensity (arrows) in the portion of the mass that appears enhanced in **a. (c)** The enhancement curve is type III, with an early peak and delayed phase washout. The vertical axis indicates the percentage of enhancement, and the horizontal axis indicates the time in seconds.

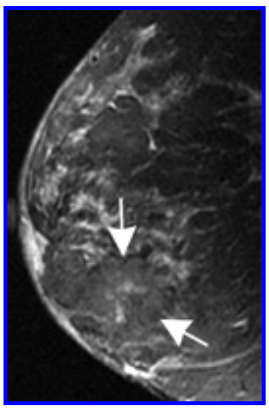

View larger version (111K):
[in this window]
[in a new window]
[Download PPT slide]

Figure 6b. Moderately to poorly differentiated palpable mass (infiltrating ductal carcinoma) in a 28-year-old woman, 3 months postpartum. **(a)** Contrast-enhanced T1-weighted fat-saturated GRE (20/4.5; flip angle, 30°) image shows an irregular mass with an irregular and spiculated margin, features typical of invasive carcinoma. **(b)** T2-weighted (4000/90) fat-saturated image shows a region of low signal intensity (arrows) in the portion of the mass that appears enhanced in **a. (c)** The enhancement curve is type III, with an early peak and delayed phase washout. The vertical axis indicates the percentage of enhancement, and the horizontal axis indicates the time in seconds.

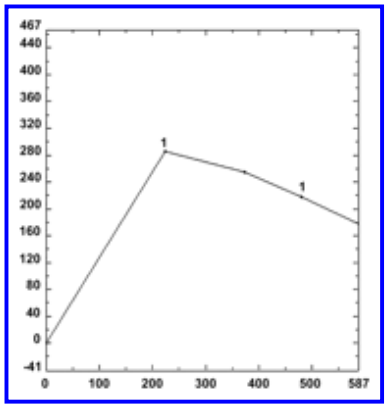

View larger version (13K):
[in this window]
[in a new window]
[Download PPT slide]

Figure 6c. Moderately to poorly differentiated palpable mass (infiltrating ductal carcinoma) in a 28-year-old woman, 3 months postpartum. **(a)** Contrast-enhanced T1-weighted fat-saturated GRE (20/4.5; flip angle, 30°) image shows an irregular mass with an irregular and spiculated margin, features typical of invasive carcinoma. **(b)** T2-weighted (4000/90) fat-saturated image shows a region of low signal intensity (arrows) in the portion of the mass that appears enhanced in **a. (c)** The enhancement curve is type III, with an early peak and delayed phase washout. The vertical axis indicates the percentage of enhancement, and the horizontal axis indicates the time in seconds.

Teaching Point The specificity of breast MR imaging is improved when both morphologic and kinetic features are considered in the interpretation (20). Because of the overlap in enhancement characteristics between benign and malignant lesions, reliance on a kinetics assessment alone is not recommended. The exclusion of cancer on the basis of persistent enhancement (a type I curve) alone would lead to false-negative results (12). The quantitative features most indicative of cancer were reported to be the maximum enhancement rate (percentage of enhancement per second) and the percentage of enhancement at 1 minute (12), with rapid enhancement being characteristic of a malignancy.

Imaging Technique

Various MR imaging protocols may be used to obtain breast images of acceptable quality. Most studies reported in the literature were performed at 1.5 T; fewer, at 1.0 T. A standard protocol includes a T2-weighted rapid (fast or turbo) spin-echo (repetition time msec/echo time msec, 4000/90; section thickness, ≤4 mm) acquisition and three-dimensional T1-weighted GRE (20/4.5; flip angle, 30°–45°; section thickness, ≤3 mm) acquisitions before and after the intravenous administration of contrast material, with the usual dose of 0.1 mmol/kg injected as a bolus and often followed by a 10–20-mL saline flush (injected manually or with a power injector). For breast imaging in the sagittal plane, an image matrix of 256 x 192 can be used with zero-filled interpolation to 512 x 512, a small field of view (16–18 cm), and chemical fat suppression. For bilateral axial breast imaging, the field of view is increased to approximately 30 cm, and high-resolution matrices (between 256 and 512) are used to reduce the voxel size.

Dedicated Breast Surface Coils

A dedicated breast surface coil should always be used. Both unilateral and bilateral coils are commercially available. Unilateral breast MR imaging typically is performed when only a two-channel coil is available; one breast can be imaged on one day, and the patient may return the next day for imaging of the contralateral breast. Most contemporary breast coils have a multicoil phased-array configuration that has been optimized for bilateral imaging of the breasts, chest wall, and axillae. Bilateral breast MR imaging is currently performed with four-channel and eight-channel coils (16-channel coils are expected to be available in the near future), with signal-to-noise improvements resulting from the higher number of channels. Bilateral imaging has the advantage of being quicker and more convenient for the patient. It also allows direct comparison between the two breasts in one field of view, thereby facilitating the assessment of symmetry during screening. However, higher spatial resolution can be obtained with unilateral breast imaging, because, for a given image matrix size, in-plane spatial resolution increases with a reduction in the field of view. It is important to select the right-to-left and superior-to-inferior directions as the phase-encoding direction for axial and sagittal acquisitions, respectively, to reduce motion artifacts. Most coils are open at the side to allow lateral access for intervention and are equipped with a compression

plate. The advantages of breast compression during imaging-guided biopsy are minimization of patient motion, decreased thickness of the breast, and shorter imaging time. However, excessive compression may compromise the enhancement of breast tumors, leading to a false-negative result (21); therefore, only minimal or no compression should be applied to immobilize the breast during routine breast MR examinations.

Contrast Enhancement

Most tumors can be detected only after intravenous contrast material administration. High-resolution T1-weighted images without or with fat saturation, with thin sections and no gap, are obtained for optimal sensitivity. These requirements are readily achieved by applying three-dimensional GRE sequences with an acquisition time of less than 2 minutes. Rapid imaging allows the application of several contrast-enhanced sequences in a single examination for simultaneous analysis of both the morphologic features and the enhancement kinetics of lesions. It is important to achieve optimal contrast between breast lesions and the surrounding glandular and fatty tissue; therefore, subtraction of unenhanced images from contrast-enhanced images is crucial. Morphologic features (Figs 7–9) are best evaluated on high-spatial-resolution images; thus, the acquisition of thin sections and the use of a small field of view are recommended (22). An analysis of architectural features can be performed at any point during the first 4 minutes 30 seconds after the contrast material injection (23).

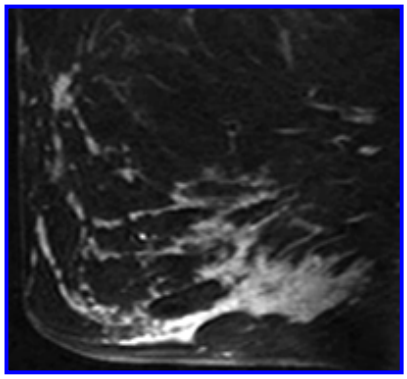

View larger version (126K):
[in this window]
[in a new window]
[Download PPT slide]

Figure 7a. Enhancement patterns in DCIS in four patients. DCIS may be manifested as stippled and clumped regional or segmental enhancement; linear and branching ductal enhancement; focal mass enhancement with spiculated, irregular, lobulated, or smooth margins; focal enhancement with a diameter of less than 5 mm; or no enhancement. **(a)** Segmental linear and reticular enhancement. **(b)** Linear enhancement. **(c)** Spiculated 1.5-cm mass within extensive sclerosing adenosis. **(d)** Small oval mass with smooth margins.

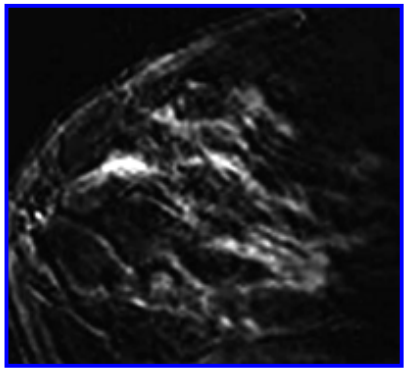

View larger version (110K):
[in this window]
[in a new window]
[Download PPT slide]

Figure 7b. Enhancement patterns in DCIS in four patients. DCIS may be manifested as stippled and clumped regional or segmental enhancement; linear and branching ductal enhancement; focal mass enhancement with spiculated, irregular, lobulated, or smooth margins; focal enhancement with a diameter of less than 5 mm; or no enhancement. **(a)** Segmental linear and reticular enhancement. **(b)** Linear enhancement. **(c)** Spiculated 1.5-cm mass within extensive sclerosing adenosis. **(d)** Small oval mass with smooth margins.

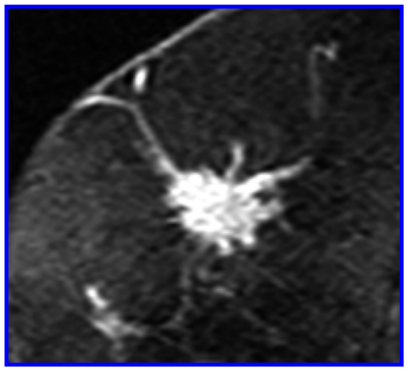

View larger version (118K):
[in this window]
[in a new window]
[Download PPT slide]

Figure 7c. Enhancement patterns in DCIS in four patients. DCIS may be manifested as stippled and clumped regional or segmental enhancement; linear and branching ductal enhancement; focal mass enhancement with spiculated, irregular, lobulated, or smooth margins; focal enhancement with a diameter of less than 5 mm; or no enhancement. **(a)** Segmental linear and reticular enhancement. **(b)** Linear enhancement. **(c)** Spiculated 1.5-cm mass within extensive sclerosing adenosis. **(d)** Small oval mass with smooth margins.

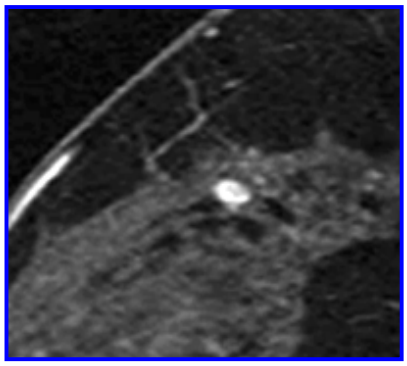

View larger version (117K):
[in this window]
[in a new window]
[Download PPT slide]

Figure 7d. Enhancement patterns in DCIS in four patients. DCIS may be manifested as stippled and clumped regional or segmental enhancement; linear and branching ductal enhancement; focal mass enhancement with spiculated, irregular, lobulated, or smooth margins; focal enhancement with a diameter of less than 5 mm; or no enhancement. **(a)** Segmental linear and reticular enhancement. **(b)** Linear enhancement. **(c)** Spiculated 1.5-cm mass within extensive sclerosing adenosis. **(d)** Small oval mass with smooth margins.

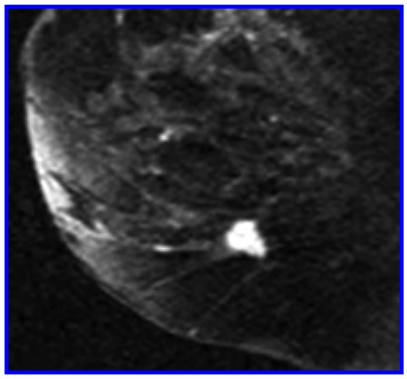

View larger version (124K):
[in this window]
[in a new window]
[Download PPT slide]

Figure 8a. Enhancement patterns in invasive ductal carcinoma in four patients. **(a)** Lobular mass with smooth margins. **(b)** Mass with spiculated margins. **(c)** Lobular mass with irregular margins. **(d)** Irregular mass associated with clumped segmental enhancement.

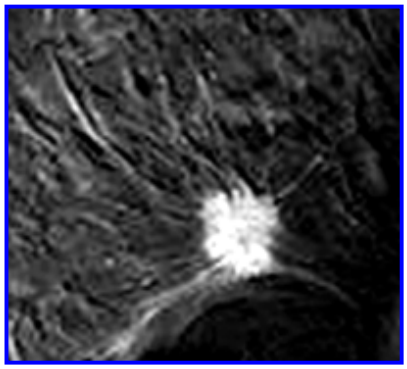

View larger version (151K):
[in this window]
[in a new window]
[Download PPT slide]

Figure 8b. Enhancement patterns in invasive ductal carcinoma in four patients. **(a)** Lobular mass with smooth margins. **(b)** Mass with spiculated margins. **(c)** Lobular mass with irregular margins. **(d)** Irregular mass associated with clumped segmental enhancement.

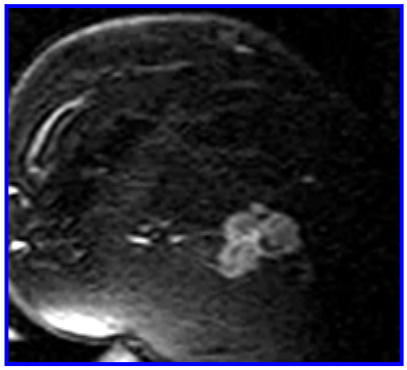

View larger version (124K):
[in this window]
[in a new window]
[Download PPT slide]

Figure 8c. Enhancement patterns in invasive ductal carcinoma in four patients. **(a)** Lobular mass with smooth margins. **(b)** Mass with spiculated margins. **(c)** Lobular mass with irregular margins. **(d)** Irregular mass associated with clumped segmental enhancement.

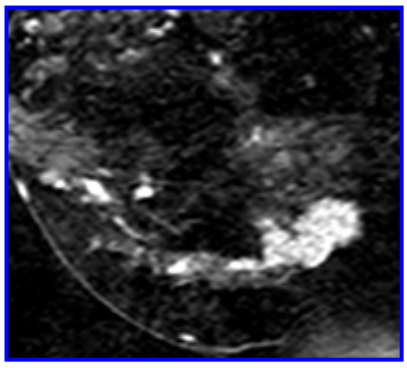

View larger version (137K):
[in this window]
[in a new window]
[Download PPT slide]

Figure 8d. Enhancement patterns in invasive ductal carcinoma in four patients. **(a)** Lobular mass with smooth margins. **(b)** Mass with spiculated margins. **(c)** Lobular mass with irregular margins. **(d)** Irregular mass associated with clumped segmental enhancement.

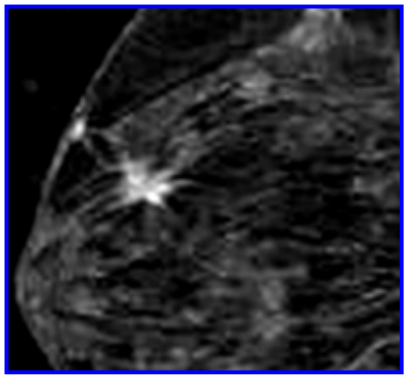

View larger version (123K):
[in this window]
[in a new window]
[Download PPT slide]

Figure 9a. Enhancement patterns in invasive lobular carcinoma in four patients. **(a)** Mass with spiculated margins. **(b)** Mass with rimlike enhancement and associated segmental clumped enhancement. **(c)** Irregular mass. **(d)** Nonmasslike regional moderate enhancement.

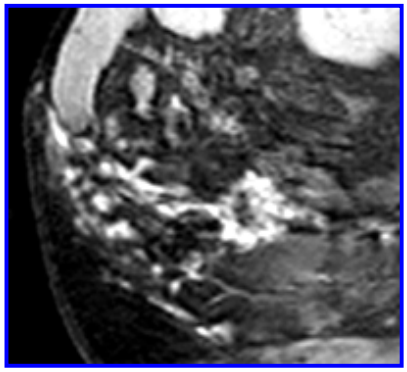

View larger version (160K):
[in this window]
[in a new window]
[Download PPT slide]

Figure 9b. Enhancement patterns in invasive lobular carcinoma in four patients. **(a)** Mass with spiculated margins. **(b)** Mass with rimlike enhancement and associated segmental clumped enhancement. **(c)** Irregular mass. **(d)** Nonmasslike regional moderate enhancement.

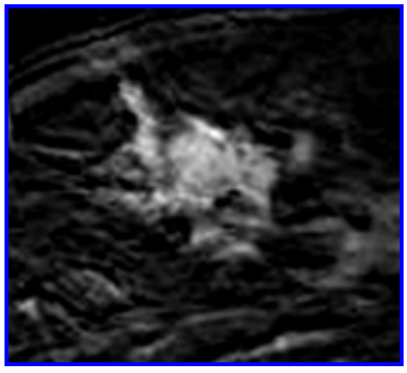

View larger version (113K):
[in this window]
[in a new window]
[Download PPT slide]

Figure 9c. Enhancement patterns in invasive lobular carcinoma in four patients. **(a)** Mass with spiculated margins. **(b)** Mass with rimlike enhancement and associated segmental clumped enhancement. **(c)** Irregular mass. **(d)** Nonmasslike regional moderate enhancement.

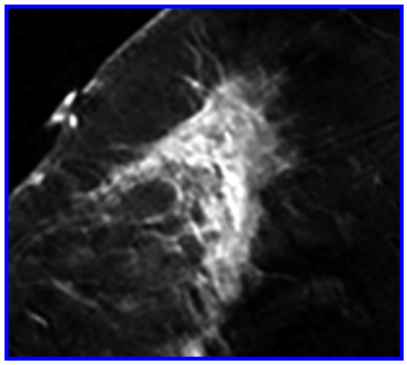

View larger version (118K):
[in this window]
[in a new window]
[Download PPT slide]

Figure 9d. Enhancement patterns in invasive lobular carcinoma in four patients. **(a)** Mass with spiculated margins. **(b)** Mass with rimlike enhancement and associated segmental clumped enhancement. **(c)** Irregular mass. **(d)** Nonmasslike regional moderate enhancement.

Trade-off between Spatial and Temporal Resolution

With increased spatial resolution (with an imaging matrix of 512 x 512) and decreased temporal resolution, the depiction of subtle morphologic details improves significantly, and improved depiction of breast lesions leads to an increase in diagnostic accuracy. There is some loss of kinetic information regarding enhancement rates (eg, the wash-in rate within the first 1–2 minutes), but, compared with morphologic features, enhancement rates are a weaker diagnostic criterion for a finding of malignancy. However, kinetic information regarding the enhancement time-course and enhancement pattern is preserved with acquisition times of 2 minutes or less (22).

Interpretation Pitfalls

Excessive Acquisition Time.— If the contrast-enhanced imaging time is longer than 2 minutes and the first contrast-enhanced images are obtained too late after peak enhancement, washout may no longer be depicted in the descending part of the signal intensity–time curve.

Excessive Size and Incorrect Placement of an ROI.— An ROI of optimal size covers only part of the lesion and should be placed in the region of strongest enhancement on the first contrast-enhanced image, a feature that is most clearly distinguishable on color maps of the maximum slope of enhancement. When an ROI is randomly placed in the mass, the enhancement curve may be variable and yield lower specificity (Fig 10).

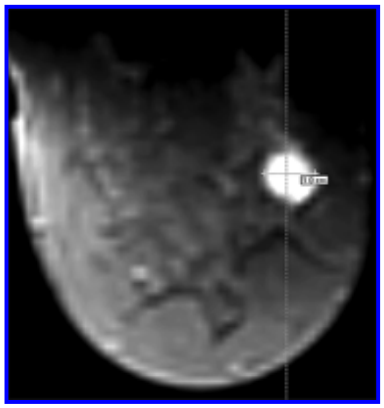

View larger version (99K):
[in this window]
[in a new window]
[Download PPT slide]

Figure 10a. Infiltrating ductal carcinoma with micropapillary features in a 52-year-old woman. **(a)** Axial contrast-enhanced T1-weighted fat-saturated GRE (20/4.5; flip angle, 30°) image shows an intensely enhanced 10-mm mass. The dotted vertical line indicates the sagittal plane in **b**. The use of multiplanar coordinates allows precise localization of masses and correlation between contrast-enhanced images and T2-weighted images. **(b)** Sagittal T2-weighted (4000/90) fat-saturated image shows an area of low signal intensity characteristic of a malignancy (arrow). Note that the dotted line is the same as the vertical coordinate in **a. (c)** Color-coded map of the maximum slope of enhancement shows that peak enhancement was off center and not covered by the ROI that was selected in the center of the mass. **(d)** Enhancement curve for the ROI in **c** shows a type II pattern. The vertical axis indicates the percentage of enhancement, and the horizontal axis indicates the time in seconds. **(e)** Color-coded map of the maximum slope of enhancement shows the ROI repositioned in the area of peak enhancement. **(f)** Enhancement curve for the ROI in **e** shows a type III washout pattern. The vertical axis indicates the percentage of enhancement, and the horizontal axis indicates the time in seconds. For the assessment of enhancement kinetics, it is important to select an ROI in the portion of the tumor with maximum peak enhancement. When an ROI is randomly placed in a mass, the enhancement curve may be variable and yield lower specificity.

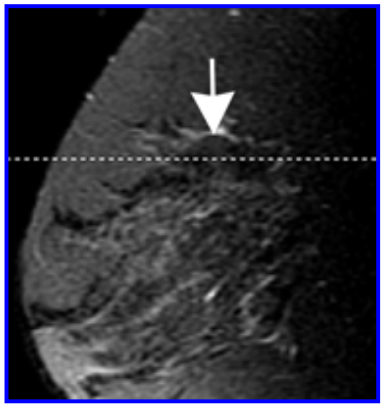

View larger version (124K):
[in this window]
[in a new window]
[Download PPT slide]

Figure 10b. Infiltrating ductal carcinoma with micropapillary features in a 52-year-old woman. **(a)** Axial contrast-enhanced T1-weighted fat-saturated GRE (20/4.5; flip angle, 30°) image shows an intensely enhanced 10-mm mass. The dotted vertical line indicates the sagittal plane in **b**. The use of multiplanar coordinates allows precise localization of masses and correlation between contrast-enhanced images and T2-weighted images. **(b)** Sagittal T2-weighted (4000/90) fat-saturated image shows an area of low signal intensity characteristic of a malignancy (arrow). Note that the dotted line is the same as the vertical coordinate in **a. (c)** Color-coded map of the maximum slope of enhancement shows that peak enhancement was off center and not covered by the ROI that was selected in the center of the mass. **(d)** Enhancement curve for the ROI in **c** shows a type II pattern. The vertical axis indicates the percentage of enhancement, and the horizontal axis indicates the time in seconds. **(e)** Color-coded map of the maximum slope of enhancement shows the ROI repositioned in the area of peak enhancement. **(f)** Enhancement curve for the ROI in **e** shows a type III washout pattern. The vertical axis indicates the percentage of enhancement, and the horizontal axis indicates the time in seconds. For the assessment of enhancement kinetics, it is important to select an ROI in the portion of the tumor with maximum peak enhancement. When an ROI is randomly placed in a mass, the enhancement curve may be variable and yield lower specificity.

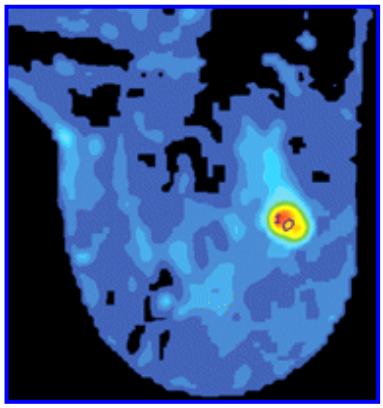

View larger version (52K):
[in this window]
[in a new window]
[Download PPT slide]

Figure 10c. Infiltrating ductal carcinoma with micropapillary features in a 52-year-old woman. **(a)** Axial contrast-enhanced T1-weighted fat-saturated GRE (20/4.5; flip angle, 30°) image shows an intensely enhanced 10-mm mass. The dotted vertical line indicates the sagittal plane in **b**. The use of multiplanar coordinates allows precise localization of masses and correlation between contrast-enhanced images and T2-weighted images. **(b)** Sagittal T2-weighted (4000/90) fat-saturated image shows an area of low signal intensity characteristic of a malignancy (arrow). Note that the dotted line is the same as the vertical coordinate in **a. (c)** Color-coded map of the maximum slope of enhancement shows that peak enhancement was off center and not covered by the ROI that was selected in the center of the mass. **(d)** Enhancement curve for the ROI in **c** shows a type II pattern. The vertical axis indicates the percentage of enhancement, and the horizontal axis indicates the time in seconds. **(e)** Color-coded map of the maximum slope of enhancement shows the ROI repositioned in the area of peak enhancement. **(f)** Enhancement curve for the ROI in **e** shows a type III washout pattern. The vertical axis indicates the percentage of enhancement, and the horizontal axis indicates the time in seconds. For the assessment of enhancement kinetics, it is important to select an ROI in the portion of the tumor with maximum peak enhancement. When an ROI is randomly placed in a mass, the enhancement curve may be variable and yield lower specificity.

Figure 10d. Infiltrating ductal carcinoma with micropapillary features in a 52-year-old woman. **(a)** Axial contrast-enhanced T1-weighted fat-saturated GRE (20/4.5; flip angle, 30°) image shows an intensely enhanced 10-mm mass. The dotted vertical line indicates the sagittal plane in **b**. The use of multiplanar coordinates allows precise localization of masses and correlation between contrast-enhanced images and T2-weighted images. **(b)** Sagittal T2-weighted (4000/90) fat-saturated image shows an area of low signal intensity characteristic of a malignancy (arrow). Note that the dotted line is the same as the vertical coordinate in **a. (c)** Color-coded map of the maximum slope of enhancement shows that peak enhancement was off center and not covered by the ROI that was selected in the center of the mass. **(d)** Enhancement curve for the ROI in **c** shows a type II pattern. The vertical axis indicates the percentage of enhancement, and the horizontal axis indicates the time in seconds. **(e)**

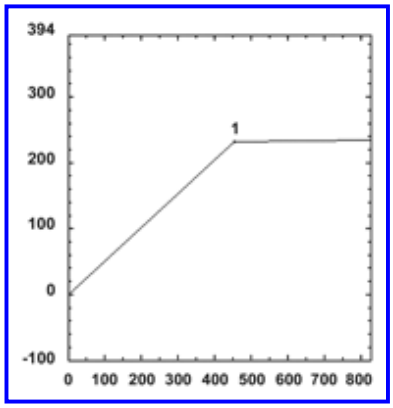

View larger version (14K):
[in this window]
[in a new window]
[Download PPT slide]

Color-coded map of the maximum slope of enhancement shows the ROI repositioned in the area of peak enhancement. **(f)** Enhancement curve for the ROI in **e** shows a type III washout pattern. The vertical axis indicates the percentage of enhancement, and the horizontal axis indicates the time in seconds. For the assessment of enhancement kinetics, it is important to select an ROI in the portion of the tumor with maximum peak enhancement. When an ROI is randomly placed in a mass, the enhancement curve may be variable and yield lower specificity.

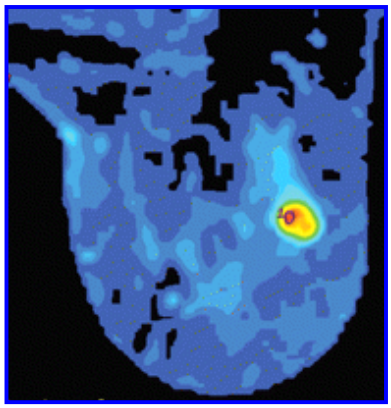

View larger version (61K):
[in this window]
[in a new window]
[Download PPT slide]

Figure 10e. Infiltrating ductal carcinoma with micropapillary features in a 52-year-old woman. **(a)** Axial contrast-enhanced T1-weighted fat-saturated GRE (20/4.5; flip angle, 30°) image shows an intensely enhanced 10-mm mass. The dotted vertical line indicates the sagittal plane in **b**. The use of multiplanar coordinates allows precise localization of masses and correlation between contrast-enhanced images and T2-weighted images. **(b)** Sagittal T2-weighted (4000/90) fat-saturated image shows an area of low signal intensity characteristic of a malignancy (arrow). Note that the dotted line is the same as the vertical coordinate in **a. (c)** Color-coded map of the maximum slope of enhancement shows that peak enhancement was off center and not covered by the ROI that was selected in the center of the mass. **(d)** Enhancement curve for the ROI in **c** shows a type II pattern. The vertical axis indicates the percentage of enhancement, and the horizontal axis indicates the time in seconds. **(e)** Color-coded map of the maximum slope of enhancement shows the ROI repositioned in the area of peak enhancement. **(f)** Enhancement curve for the ROI in **e** shows a type III washout pattern. The vertical axis indicates the percentage of enhancement, and the horizontal axis indicates the time in seconds. For the assessment of enhancement kinetics, it is important to select an ROI in the portion of the tumor with maximum peak enhancement. When an ROI is randomly placed in a mass, the enhancement curve may be variable and yield lower specificity.

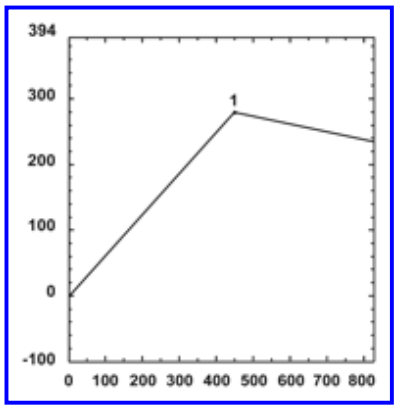

View larger version (15K):
[in this window]
[in a new window]
[Download PPT slide]

Figure 10f. Infiltrating ductal carcinoma with micropapillary features in a 52-year-old woman. **(a)** Axial contrast-enhanced T1-weighted fat-saturated GRE (20/4.5; flip angle, 30°) image shows an intensely enhanced 10-mm mass. The dotted vertical line indicates the sagittal plane in **b**. The use of multiplanar coordinates allows precise localization of masses and correlation between contrast-enhanced images and T2-weighted images. **(b)** Sagittal T2-weighted (4000/90) fat-saturated image shows an area of low signal intensity characteristic of a malignancy (arrow). Note that the dotted line is the same as the vertical coordinate in **a. (c)** Color-coded map of the maximum slope of enhancement shows that peak enhancement was off center and not covered by the ROI that was selected in the center of the mass. **(d)** Enhancement curve for the ROI in **c** shows a type II pattern. The vertical axis indicates the percentage of enhancement, and the horizontal axis indicates the time in seconds. **(e)** Color-coded map of the maximum slope of enhancement shows the ROI repositioned in the area of peak enhancement. **(f)** Enhancement curve for the ROI in **e** shows a type III washout pattern. The vertical axis indicates the percentage of enhancement, and the horizontal axis indicates the time in seconds. For the assessment of enhancement kinetics, it is important to select an ROI in the portion of the tumor

with maximum peak enhancement. When an ROI is randomly placed in a mass, the enhancement curve may be variable and yield lower specificity.

Complex Imaging Findings (Physiologic or Postoperative Changes).— Areas of normal parenchyma in premenopausal women may appear focally enhanced, a feature that may lead to a false-positive finding. Transiently enhancing foci have been observed in the breasts of many healthy women, especially during the second half of the menstrual cycle. Therefore, to minimize false-positive results, breast imaging should be performed during the first half of the menstrual cycle (days 3–14) (24).

In the evaluation of small lesions, the use of multiplanar coordinates allows precise localization of masses and correlation between contrast-enhanced images and T2-weighted images (Fig 10). Otherwise, small masses may be difficult to map on images obtained with the different sequences.

Breast MR imaging for the postoperative assessment of residual disease should be performed 28 days or more after surgery (25). The time interval between surgery and MR imaging of the breast has the greatest influence on the specificity and NPV of MR imaging, which increase progressively over time. However, patients with positive surgical margins whose further surgery should not be delayed may benefit from immediate postoperative MR imaging to determine the distance of disease extension from the surgical site. Future research will provide more data about optimal postoperative management. Postoperative sites may appear enhanced up to 6 months after surgery without radiation therapy and up to 18–24 months after radiation therapy (5). MR imaging may not be useful for excluding small foci of residual disease, but it may be helpful for identifying gross residual disease or unsuspected multifocality or multicentricity of disease. Findings suggestive of residual tumor include thickening beyond 5 mm of the enhanced wall of the seroma, and an irregular or nodular enhanced rim around the resection cavity (25). Lack of enhancement at the lumpectomy site does not obviate reexcision if the surgical margin is positive.

Indications for Breast MR Imaging

Several indications for contrast-enhanced breast MR imaging have been identified and evaluated (5). MR imaging is useful for screening of selected patient populations and for problem solving, therapy planning, and follow-up. For screening, breast MR imaging is used in patients with a high risk of breast cancer (*BRCA1* or *BRCA2* mutation carriers), a strong family history of breast cancer, or a condition that may impair mammographic interpretation (eg, silicone or nonsilicone breast augmentation or radiographically dense breasts). In women with a familial risk of breast cancer (lifetime risk of 20% or more), MR imaging was shown to have the highest sensitivity, specificity, and PPV for the detection of invasive as well as of intraductal cancer when compared with mammography and breast US (26). MR imaging may be performed for contralateral breast screening in women who are newly diagnosed with breast cancer, to search for an occult primary lesion in women with axillary metastases, and in women with previous biopsy-proved atypia or lobular carcinoma in situ. MR imaging may be used for diagnostic work-up in patients with problematic mammograms, especially for lesions seen on only one view, to determine the local extent of malignancy and chest wall involvement, and for preoperative staging. The size of the primary tumor and the presence of multifocal or multicentric disease are important considerations when breast-conserving therapy is planned. After lumpectomy, MR imaging may be performed to identify any residual disease, especially when a positive margin was detected at histopathologic analysis. MR imaging also has been used to assess the response to neoadjuvant chemotherapy. In patients with histologically proved invasive lobular carcinoma, MR imaging is helpful for evaluating the extent, multifocality, and multicentricity of disease, features that are difficult to assess with a physical examination or mammography. In patients with histologically proved infiltrating ductal carcinoma, particularly those who desire breast-conserving therapy, MR imaging may be used to evaluate the extent of disease. In those for whom mastectomy is being considered, MR imaging may be used to determine whether chest wall invasion is present. MR imaging may play a role in ongoing disease management, when recurrence is suspected, and when clinical and mammographic findings are inconclusive, or when there is a recurrence of breast cancer in a patient with postoperative tissue reconstruction (eg, with tissue transfer flaps). Another important indication for MR imaging is to differentiate between postoperative scar tissue and recurrent tumor.

Future Developments

Novel MR imaging methods that have the potential to improve specificity for the identification of breast malignancy include multiparametric MR imaging, proton MR spectroscopic imaging, and sodium (Na-23) MR imaging. When used in combination, these techniques provide a comprehensive data set that has far better potential for increasing the accuracy of diagnosis of breast disease than would any single measure. A combination of MR imaging, MR spectroscopy, and sodium MR imaging parameters may be examined in a single MR study (9,10). Multiparametric MR imaging (with unenhanced T1-weighted, T2-weighted, and contrast-enhanced T1-weighted sequences), combined with MR spectroscopic imaging or sodium MR imaging and advanced computer-aided methods such as the iterative self-organizing data analysis (ISODATA) algorithm, can greatly assist the radiologist in the detection and classification of breast lesions (27). The combination of these different MR imaging techniques allows the integration of molecular imaging data with diagnostic imaging data. MR spectroscopic imaging can depict changes in the concentration of intracellular metabolites such as choline, a recognized marker for malignant tissue (28) or increased membrane turnover. Investigators in several studies have demonstrated the detectability of choline in malignant breast lesions with the use of single-voxel proton MR spectroscopy (29) and with multivoxel spectroscopy (10, 30). A high choline concentration appears to be the spectroscopic hallmark not only of breast cancer but also of human brain tumors, and some investigators have reported a correlation between the tumor grade and choline concentration (31). High choline concentrations also are considered a marker for prostate cancer (32) and head and neck cancers (33). Sodium is abundant in most tissues and is actively pumped out of healthy cells by Na^+-H^+–adenosine triphosphatase, which maintains a large difference in sodium concentration across the cell membrane at the cost of energy-rich adenosine triphosphate. An increase in the total sodium concentration in tissue may be indicative of compromised cellular membrane integrity, impaired energy metabolism, or increased interstitial space through a change in cellular organization or an increase in the vascular volume, all of which are observed in tumors. Tumor growth is accompanied by a change in Na^+-H^+ exchange kinetics, which is part of the signaling mechanism that initiates cell division, and sometimes also by an impaired energy metabolism. The resultant increase in intracellular sodium adds to the increase in the total sodium concentration because of increased interstitial space and neovascularization. The sodium exchange across the cell membrane also may be altered by changes in intra- or extracellular pH, as those affect the activity of the Na^+-H^+ exchange proteins. Typically, intracellular acidification is a by-product of a failure of the energy metabolism, and it causes the augmentation of influx of sodium due to reduced Na^+-H^+–adenosine triphosphatase activity. The intracellular sodium cannot be imaged separately from the extracellular sodium concentration without the use of sophisticated MR methods. However, the total sodium concentration in tissue can be resolved by using MR imaging (34,35). The ISODATA approach allows the superimposition of a map of combined choline and sodium concentrations over the enhancing breast tissue to enable a characterization of breast lesions, as illustrated in Figure 11.

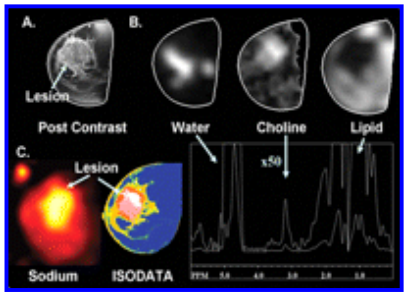

View larger version (54K):
[in this window]
[in a new window]
[Download PPT slide]

Figure 11. Invasive lobular carcinoma in a 43-year-old woman. Multiparametric ISODATA cluster analysis map shows overlap of sodium and proton MR spectroscopic data corresponding to the enhanced mass. In *A.*, the contrast-enhanced image shows a heterogeneously enhanced mass with irregular margins. *B.*, Metabolite maps of water, choline, and lipids. *C.*, Sodium MR image and corresponding ISODATA feature map. Spectra show a choline concentration of 3.2 ppm with a signal-to-noise ratio of 10.6 and an approximately 50% increase in the tissue sodium concentration in the region of pathologically proved cancer.

Summary

Top
Abstract
LEARNING OBJECTIVES
Introduction
Enhancement Patterns
Other Features
Enhancement Kinetics
Imaging Technique
Indications for Breast MR...
Future Developments
Summary
References

Teaching Point In classifying breast lesions, the assessment of margin and qualitative enhancement intensity (at 2 minutes or less after contrast material injection) are the most important features currently available for breast mass characterization. The next most important feature is the qualitative assessment of the enhancement kinetics curve. The absence of enhancement is associated with an NPV of 88% for cancer. The relative risk of cancer for a lesion that has a washout curve is five times higher than that for a lesion that has a persistent curve. However, a persistent kinetics curve was reported in 45% of malignant lesions (12). The specificity of breast MR imaging is improved when both morphologic and kinetic features are considered in the image interpretation; therefore, the breast MR imaging technique should be optimized to achieve high spatial and temporal resolution.

Acknowledgments

The authors thank Denise R. Schmidt, MD, for her assistance with the case selection.

Footnotes

Abbreviations: DCIS = ductal carcinoma in situ, GRE = gradient echo, ISODATA = iterative self-organizing data analysis, NPV = negative predictive value, PPV = positive predictive value, ROI = region of interest

References

Top
Abstract
LEARNING OBJECTIVES
Introduction
Enhancement Patterns
Other Features
Enhancement Kinetics
Imaging Technique
Indications for Breast MR...
Future Developments
Summary
References

1. Fischer U, Kopka L, Grabbe E. Breast carcinoma: effect of preoperative contrast-enhanced MR imaging on the therapeutic approach. Radiology 1999;213:881–888.[Abstract/Free Full Text]
2. Kuhl CK, Schmutzler RK, Leutner CC, et al. Breast MR imaging screening in 192 women proved or suspected to be carriers of a breast cancer susceptibility gene: preliminary results. Radiology 2000;215:267–279.[Abstract/Free Full Text]
3. Morris EA, Schwartz LH, Dershaw DD, Van Zee KJ, Abramson AF, Liberman L. MR imaging of the breast in patients with occult primary breast carcinoma. Radiology 1997;205:437–440.[Abstract]
4. Slanetz PJ, Edmister WB, Yeh ED, Talele AC, Kopans DB. Occult contralateral breast carcinoma incidentally detected by breast magnetic resonance imaging. Breast J 2002;8:145–148.[Medline]
5. Lee CH. Problem solving MR imaging of the breast. Radiol Clin North Am 2004;42:919–934.[Medline]
6. Bluemke DA, Gatsonis CA, Chen MH, et al. Magnetic resonance imaging of the breast prior to biopsy. JAMA 2004;292:2735–2742.[Abstract/Free Full Text]
7. Ikeda DM, Birdwell RL, Daniel BL. Potential role of magnetic resonance imaging and other modalities in ductal carcinoma in situ detection. Magn Reson Imaging Clin N Am 2001;9:345–356, vii.[Medline]
8. American College of Radiology. Breast imaging reporting and data system (BI-RADS). 4th ed. Reston, Va: American College of Radiology, 2003.
9. Jacobs MA, Ouwerkerk R, Wolff AC, et al. Multiparametric and multinuclear magnetic resonance imaging of human breast

cancer: current applications. Technol Cancer Res Treat 2004;3:543–550.[Medline]

10. Jacobs MA, Barker PB, Argani P, Ouwerkerk R, Bhujwalla ZM, Bluemke DA. Combined dynamic contrast enhanced breast MR and proton spectroscopic imaging: a feasibility study. J Magn Reson Imaging 2005;21:23–28.[Medline]
11. Leinsinger G, Schlossbauer T, Scherr M, Lange O, Reiser M, Wismuller A. Cluster analysis of signal-intensity time course in dynamic breast MRI: does unsupervised vector quantization help to evaluate small mammographic lesions? Eur Radiol 2006;16(5):1138–1146.[Medline]
12. Schnall MD, Blume J, Bluemke DA, et al. Diagnostic architectural and dynamic features at breast MR imaging: multicenter study. Radiology 2006; 238:42–53.[Abstract/Free Full Text]
13. Nunes LW, Schnall MD, Orel SG. Update of breast MR imaging architectural interpretation model. Radiology 2001;219:484–494.[Abstract/Free Full Text]
14. Kuhl CK, Bieling HB, Gieseke J, et al. Healthy premenopausal breast parenchyma in dynamic contrast-enhanced MR imaging of the breast: normal contrast medium enhancement and cyclical-phase dependency. Radiology 1997;203:137–144.[Abstract]
15. Malich A, Fischer DR, Wurdinger S, et al. Potential MRI interpretation model: differentiation of benign from malignant breast masses. AJR Am J Roentgenol 2005;185:964–970.[Abstract/Free Full Text]
16. Ikeda DM, Hylton NM, Kinkel K, et al. Development, standardization, and testing of a lexicon for reporting contrast-enhanced breast magnetic resonance imaging studies. J Magn Reson Imaging 2001;13:889–895.[Medline]
17. Kawashima M, Tamaki Y, Nonaka T, et al. MR imaging of mucinous carcinoma of the breast. AJR Am J Roentgenol 2002;179:179–183.[Abstract/Free Full Text]
18. Kuhl CK, Klaschik S, Mielcarek P, Gieseke J, Wardelmann E, Schild HH. Do T2-weighted pulse sequences help with the differential diagnosis of enhancing lesions in dynamic breast MRI? J Magn Reson Imaging 1999;9:187–196.[Medline]
19. Kuhl CK, Mielcareck P, Klaschik S, et al. Dynamic breast MR imaging: are signal intensity time course data useful for differential diagnosis of enhancing lesions? Radiology 1999;211:101–110.[Abstract/Free Full Text]
20. Schnall MD, Rosen S, Englander S, Orel SG, Nunes LW. A combined architectural and kinetic interpretation model for breast MR images. Acad Radiol 2001;8:591–597.[Medline]
21. Kuhl CK, Elevelt A, Leutner CC, Gieseke J, Pakos E, Schild HH. Interventional breast MR imaging: clinical use of a stereotactic localization and biopsy device. Radiology 1997;204:667–675.[Abstract]
22. Kuhl CK, Schild HH, Morakkabati N. Dynamic bilateral contrast-enhanced MR imaging of the breast: trade-off between spatial and temporal resolution. Radiology 2005;236:789–800.[Abstract/Free Full Text]
23. Nunes LW, Englander SA, Charafeddine R, Schnall MD. Optimal post-contrast timing of breast MR image acquisition for architectural feature analysis. J Magn Reson Imaging 2002;16:42–50.[Medline]
24. Delille JP, Slanetz PJ, Yeh ED, Kopans DB, Garrido L. Physiologic changes in breast magnetic resonance imaging during the menstrual cycle: perfusion imaging, signal enhancement, and influence of the T1 relaxation time of breast tissue. Breast J 2005;11(4):236–241.[Medline]
25. Frei KA, Kinkel K, Bonel HM, Lu Y, Esserman LJ, Hylton NM. MR imaging of the breast in patients with positive margins after lumpectomy: influence of the time interval between lumpectomy and MR imaging. AJR Am J Roentgenol 2000; 175:1577–1584.[Abstract/Free Full Text]
26. Kuhl CK, Schrading S, Leutner CC, et al. Mammography, breast ultrasound, and magnetic resonance imaging for surveillance of women at high familial risk for breast cancer. J Clin Oncol 2005; 23:8469–8476.[Abstract/Free Full Text]
27. Jacobs MA, Barker PB, Bluemke DA, et al. Benign and malignant breast lesions: diagnosis with multiparametric MR imaging. Radiology 2003; 229:225–232.[Abstract/Free Full Text]
28. Bolan PJ, Meisamy S, Baker EH, et al. In vivo quantification of choline compounds in the breast with 1H MR spectroscopy. Magn Reson Med 2003;50:1134–1143.[Medline]
29. Gribbestad IS, Singstad TE, Nilsen G, et al. In vivo 1H MRS of normal breast and breast tumors using a dedicated double breast coil. J Magn Reson Imaging 1998;8:1191–1197.[Medline]
30. Jacobs MA, Barker PB, Bottomley PA, Bhujwalla Z, Bluemke DA. Proton magnetic resonance spectroscopic imaging of human breast cancer: a preliminary study. J Magn Reson Imaging 2004;19: 68–75.[Medline]
31. Calvar JA, Meli FJ, Romero C, et al. Characterization of brain tumors by MRS, DWI and Ki-67 labeling index. J Neurooncol 2005;72:273–280.[Medline]
32. Kurhanewicz J, Vigneron DB, Nelson SJ, et al. Citrate as an in vivo marker to discriminate prostate cancer from benign prostatic hyperplasia and normal prostate peripheral zone: detection via localized proton spectroscopy. Urology 1995;45: 459–466.[Medline]
33. Mukherji SK, Schiro S, Castillo M, Kwock L, Muller KE, Blackstock W. Proton MR spectroscopy of squamous cell carcinoma of the extracranial head and neck: in vitro and in vivo studies. AJNR Am J Neuroradiol 1997;18:1057–1072. [Abstract]
34. Thulborn KR, Davis D, Adams H, Gindin T, Zhou J. Quantitative tissue sodium concentration mapping of the growth of focal cerebral tumors with sodium magnetic resonance imaging. Magn Reson Med 1999;41:351–359.[Medline]

35. Ouwerkerk R, Bleich KB, Gillen JS, Pomper MG, Bottomley PA. Tissue sodium concentration in human brain tumors as measured with 23Na MR imaging. Radiology 2003;227:529–537.[Abstract/Free Full Text]